

Large Hadron Collider reach for supersymmetric models with compressed mass spectra

Thomas J. LeCompte¹ and Stephen P. Martin^{2,3}

1) *Argonne National Laboratory, Argonne IL 60439, USA*

2) *Department of Physics, Northern Illinois University, DeKalb IL 60115, USA*

3) *Fermi National Accelerator Laboratory, P.O. Box 500, Batavia IL 60510, USA*

Many theoretical and experimental results on the reach of the Large Hadron Collider are based on the mSUGRA-inspired scenario with universal soft supersymmetry breaking parameters at the apparent gauge coupling unification scale. We study signals for supersymmetric models in which the sparticle mass range is compressed compared to mSUGRA, using cuts like those employed by ATLAS for 2010 data. The acceptance and the cross-section times acceptance are found for several model lines that employ a compression parameter to smoothly interpolate between the mSUGRA case and the extreme case of degenerate gaugino masses at the weak scale. For models with moderate compression, the reach is not much worse, and can even be substantially better, than the mSUGRA case. For very compressed mass spectra, the acceptances are drastically reduced, especially when a more stringent effective mass cut is chosen.

Contents

I. Introduction	2
II. Procedures and signal requirements	3
III. Results for several classes of compressed SUSY models	5
A. Models with light squarks and winos	5
B. Models with heavy winos	10
C. Models with heavy squarks	13
D. Models with light stops motivated by dark matter	16
IV. Outlook	18
References	18

I. INTRODUCTION

The continuing explorations of the ATLAS [1] and CMS [2] experiments at the Large Hadron Collider (LHC) are testing the idea that supersymmetry [3] (SUSY) is the solution to the hierarchy problem associated with the small ratio of the electroweak scale to the Planck scale and other high energy scales. Already, there are significant bounds from both ATLAS [4]-[7] and CMS [8]-[10] on certain supersymmetric models, especially those formulated in terms of universal soft supersymmetry-breaking parameters at the scale of apparent gauge coupling unification, the so-called “mSUGRA” or “CMSSM” scenario. However, the essential idea of supersymmetry is simply that of a symmetry connecting fermion and boson degrees of freedom, and the unknown features of the supersymmetry breaking mechanism allow for a much more diverse variety of possibilities. It is therefore always important to consider the extent to which the limits obtained from experimental searches depend on the specific model assumptions.

The input parameters for mSUGRA models are a universal gaugino mass $M_{1/2}$, a universal scalar mass m_0 , a common scalar cubic coupling parameter A_0 , the ratio of the Higgs vacuum expectation values $\tan\beta = \langle v_u \rangle / \langle v_d \rangle$, and the sign of the supersymmetric Higgs mass parameter μ . Existing model-dependent LHC searches exploit the fact that supersymmetric particle production and decay in mSUGRA-like models typically result in both energetic jets from gluino or squark decays and large missing transverse energy E_T^{miss} due to the presence in each superpartner decay chain of a neutral, weakly-interacting, stable lightest supersymmetric particle (LSP). In mSUGRA models, there is typically a hierarchy of a factor of 6 or so between the masses of the gluino and the neutralino LSP, leading to robust signals. Along with the gluino, the dominant production mechanisms involve squarks, which are never much lighter than the gluino in viable mSUGRA models.

If the supersymmetric mass spectrum is compressed, that is, if ratio of the mass scale of the strongly interacting superpartners (the gluino and squarks) and the LSP mass is smaller, then one may expect that the detection efficiency and acceptance will be lowered, because there will often be less energetic jets and leptons from the decays, as well as less E_T^{miss} . Cuts on the relevant kinematic quantities are necessary for triggering and for reduction of backgrounds, so that a sufficiently compressed supersymmetric mass spectrum will have greatly reduced discovery potential even if there is a large production cross-section. The purpose of this paper is to study this issue quantitatively, using as an example selections employed by ATLAS in the study of 35 pb⁻¹ of data collected in 2010 at $\sqrt{s} = 7$ TeV [4]-[7]. Other recent[†] studies of non-mSUGRA scenarios at the LHC from other viewpoints can be found, for example, in [12]-[18].

In this paper we are interested in the consequences of a compressed superpartner mass spectrum rather than the model-building ideas that might be involved in such a scenario. However, it is worth noting that in non-mSUGRA models, it is perfectly sensible to choose the three gaugino mass parameters to be in any desired proportion at the apparent gauge coupling unification scale, which in turn allows any desired ratio of gaugino masses at the TeV scale after renormalization group

[†] The reduced reach of hadron colliders for compressed superpartner mass spectra was studied as long ago as the mid-1980s [11], in the context of < 100 GeV gluino searches by the UA1 detector at the CERN SPS $p\bar{p}$ collider.

running. A huge number of different model building ideas can realize this, and one restricted class will be mentioned in subsection IIID below. Similarly, the squark and slepton mass parameters can be chosen arbitrarily, with no problems as long as flavor symmetries are respected (as we do in this paper).

The rest of this paper is organized as follows. Section II describes our procedures. Section III presents results on the acceptance and on the cross-section times acceptance, for several classes of models defined with a compression parameter that can be continuously dialed to vary the ratio of gluino to LSP masses. Subsection IIIA gives results for models with light squarks and winos, subsection IIIB for similar models but with the wino mass parameter taken to be large enough so that the squarks and gluino do not decay to wino-like intermediate states, and subsection IIIC similarly discusses models that have heavy squarks. All of these are complete SUSY models, but are defined without reference to dark matter or other indirect observable clues on the superpartner spectrum. In section IIID, we discuss reach for a class of compressed SUSY models that have relatively light top squarks and are specifically motivated by the dark matter relic abundance inferred from WMAP and other experiments. Section IV contains some concluding remarks.

II. PROCEDURES AND SIGNAL REQUIREMENTS

For this paper, we used **MadGraph/MadEvent 4.4.62** [19] to generate hard scattering events using **CTEQ6L1** [20] parton distribution functions, **Pythia 6.422** [21] for decays and showering and hadronization, and **PGS 4** [22] for detector simulation. In compressed SUSY models, it is potentially important to match correctly (without overcounting) between matrix-element and showering/hadronization software generation of additional jets. We do this by generating each lowest-order process together with the same process with one additional jet at the matrix-element level, followed by MLM matching with P_T -ordered showers with the shower- K_T scheme with $Q_{\text{cut}} = 100$ GeV, as described in [23] and implemented in the MadGraph/MadEvent package. (Including up to two extra jets at the matrix-element level is much more time-consuming, and we found with some sample testing that even for very compressed superpartner mass spectra it did not make a significant difference with our setup.) For the detector simulation, we used the default ATLAS-like parameter card file provided with the PGS distribution, but with a jet cone size of $\Delta R = 0.4$. Cross-sections were normalized to the next-to-leading order output of **Prospino 2.1** [24].

To define signals, we follow (a slightly simplified version of) the ATLAS cuts A, C, D for multijets+ E_T^{miss} from ref. [5], and the single lepton plus multijets+ E_T^{miss} signal from ref. [4], called L here. (We do not attempt to simulate the ref. [5] signal region B, which involves the kinematic variable m_{T2} . The B region is intended to be intermediate between the A and D regions.) The signal requirements are as follows. The minimum number of jets is 2 for signal A and 3 for signals C, D, and L, each with $p_T > 40$ GeV for A, C, D and $p_T > 30$ GeV for L. These jets must have $|\eta| < 2.5$. The p_T of the leading jet must exceed 120 GeV for A, C, D, and 60 GeV for L. The required number of leptons $\ell = (e, \mu)$ is exactly 0 for A, C, D and exactly 1 for L. Here leptons are defined to have $|\eta| < 2.4$ (2.47) for muons (electrons), and $p_T^\ell > 10$ GeV in signals A, C, D and $p_T^\ell > 20$ GeV in signal L, and to be farther than $\Delta R = \sqrt{(\Delta\eta)^2 + (\Delta\phi)^2} > 0.4$ from the nearest jet

	A	C	D	L
Number of jets	≥ 2	≥ 3	≥ 3	≥ 3
Leading jet p_T [GeV]	> 120	> 120	> 120	> 60
Other jet(s) p_T [GeV]	> 40	> 40	> 40	> 30
$\Delta\phi(\vec{p}_T^{\text{miss}}, j_{1,2,3})$	> 0.4	> 0.4	> 0.4	> 0.2
m_{eff} [GeV]	> 500	> 500	> 1000	> 500
$E_T^{\text{miss}}/m_{\text{eff}}$	> 0.3	> 0.25	> 0.25	> 0.25
Number of leptons	$= 0$	$= 0$	$= 0$	$= 1$
Lepton p_T [GeV]	–	–	–	> 20
m_T [GeV]	–	–	–	> 100
ATLAS $\sigma \times \text{Acc}$ [pb]	< 1.3	< 1.1	< 0.11	< 0.138

TABLE I: Summary of cuts for the signals A, C, D, L simulated here, following ATLAS 2010 data analyses [4, 5]. Also shown on the last line are the ATLAS 95% CL bounds from 2010 data (35 pb^{-1} at $\sqrt{s} = 7 \text{ TeV}$) on the non-Standard Model contribution to the cross-section times acceptance in the four signal regions.

candidate with $|\eta| < 4.9$ and $p_T > 20 \text{ GeV}$. The effective mass m_{eff} is defined as the scalar sum of the E_T^{miss} and the p_T 's of: the leading 2 jets for A; the leading 3 jets for C, D; and the leading three jets and the leading lepton for L. The A, C, D, L signals require $m_{\text{eff}} > 500, 500, 1000, 500 \text{ GeV}$ respectively. The missing transverse energy E_T^{miss} must exceed a fraction of m_{eff} in each event, given by 0.3 for A and 0.25 for C, D, L. For the A, C, D signals, the jets with $p_T > 40 \text{ GeV}$, up to a maximum of 3, are required to be isolated from the missing transverse momentum according to $\Delta\phi(\vec{p}_T^{\text{miss}}, j) > 0.4$. A similar but weaker requirement applies to L: $\Delta\phi(\vec{p}_T^{\text{miss}}, j) > 0.2$ for the three highest- p_T jets. For signal L only, the transverse mass $m_T = \sqrt{2(p_T^\ell E_T^{\text{miss}} - \vec{p}_T^\ell \cdot \vec{p}_T^{\text{miss}})}$ is required to exceed 100 GeV for the single lepton ℓ .

These signal requirements are summarized in Table I. Note that these cuts automatically imply a lower limit on E_T^{miss} of 150, 125, 250, and 125 GeV for signals A, C, D, and L, respectively.

The ATLAS searches using the 2010 data (35 pb^{-1} at $\sqrt{s} = 7 \text{ TeV}$) in [4, 5] were given in terms of a grid of mSUGRA models with $\tan\beta = 3$ and $A_0 = 0$ (which in the mSUGRA framework are ruled out already based on the LEP searches for a scalar Higgs boson). A realistic estimate of the relevant backgrounds would require a dedicated analysis taking into account specific detailed features of the LHC detectors, and will not be attempted here. We will therefore present results only for the SUSY signals after the cuts listed above. However, ATLAS has also presented limits on non-Standard-Model contributions to the $\sigma \times \text{acceptance}$ as $< (1.3, 1.1, 0.11, \text{ and } 0.138) \text{ pb}$ for signals (A,C,D,L) respectively. These can be considered model-independent, with the caveat that supersymmetry, if present, could contribute to the control regions used to estimate backgrounds from data in different ways depending on the superpartner masses and decays. Also, it is very likely that future searches will use modified signal requirements in order to extend the reach.

Since our tools for generating events and simulating detector response are not the same as those used by ATLAS, the cross-section and acceptance results found below clearly cannot be interpreted in exact correspondence to the ATLAS ones. However, we have checked that the results of our analysis methods correlate well to those in refs. [4, 5] for the grid of mSUGRA models used there. For the all-jets signals A,C,D, we find cross-section times acceptances that typically agree with the

ATLAS results (as given in Figures 17a,c,d of the web site referred to by [5]) to 20% or better, with some fluctuations that appear to be statistical in nature. For the 1-lepton signal L, our results for the acceptance are similar but tend to be systematically higher than those found in Figures 6a,b of the web site referred to by [4], by typically 20% to 50%, again with significant statistical fluctuations. Keeping these in mind, at least an approximate estimate of the true detector response may be gleaned from the results below, and the general trends should be robust.

III. RESULTS FOR SEVERAL CLASSES OF COMPRESSED SUSY MODELS

A. Models with light squarks and winos

In this section, we consider a model framework featuring a quantity c that parameterizes the compression of the supersymmetric mass spectrum. Specifically, we parameterize the electroweak gaugino mass parameters at the TeV scale in terms of the gluino physical mass as:

$$M_1 = \left(\frac{1+5c}{6} \right) M_{\tilde{g}}, \quad M_2 = \left(\frac{1+2c}{3} \right) M_{\tilde{g}}. \quad (3.1)$$

The value $c = 0$ gives an mSUGRA-like mass spectrum with gaugino masses equal at $M_{\text{GUT}} = 2.5 \times 10^{16}$ GeV, and $c = 1$ gives a completely compressed spectrum in which the gluino, wino, and bino masses are equal at the TeV scale. The gluino mass $M_{\tilde{g}}$ is treated as a variable input parameter. We also select $\tan\beta = 10$ and positive $\mu = M_{\tilde{g}} + 200$ GeV to compute the physical masses of charginos \tilde{C}_i and neutralinos \tilde{N}_i . The first- and second-family squark masses are:

$$m_{\tilde{u}_R} = m_{\tilde{d}_R} = m_{\tilde{u}_L} = 0.96M_{\tilde{g}}, \quad m_{\tilde{d}_L}^2 = m_{\tilde{u}_L}^2 - \cos(2\beta)m_W^2, \quad (3.2)$$

and sleptons are degenerate with the squarks (so too heavy to appear in chargino and neutralino two-body decays). The top squark masses are taken to be $m_{\tilde{t}_1} = M_{\tilde{g}} - 160 + c(180 - 0.09M_{\tilde{g}})$ and $m_{\tilde{t}_2} = M_{\tilde{g}} + 25$, in GeV. The lightest Higgs mass is fixed at $m_{h^0} = 115$ GeV, and the heavier Higgs masses with $m_{A^0} = 0.96M_{\tilde{g}}$. These values are engineered to provide relatively smoothly varying branching ratios as the compression parameter c is varied, although transitions of \tilde{N}_2 and \tilde{C}_1 decays from on-shell to off-shell weak bosons are inevitable as the compression increases. The choices for $\tan\beta$ and μ are essentially arbitrary, and not very much would change if they were modified (within some reasonable range). The reason for the choice for the parameterization of the stop masses was just to avoid suddenly turning on or off any 2-body decay modes as the parameter c is varied within each model line, notably by making sure that the the gluinos cannot decay to stops by kinematics along the entire model line. The masses of the most relevant superpartners are shown in Figure 1 for the case $M_{\tilde{g}} = 700$ GeV, illustrating the effect of the compression parameter c on the spectrum. An orthogonal direction in parameter space is obtained by varying $M_{\tilde{g}}$, which moves the entire mass spectrum up or down for fixed c .

In these models, gluino and squark production dominate at the LHC. The gluino decays mostly by the two-body mode $\tilde{g} \rightarrow \bar{q}q$ or $q\bar{q}$, and right-handed squarks decay mostly directly to the

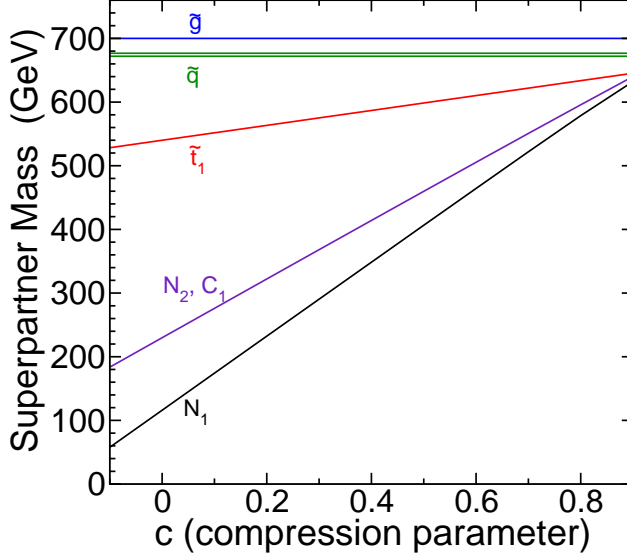


FIG. 1: The masses of the most relevant superpartners for the class of models defined in subsection III A, as a function of the compression parameter c , for fixed $M_{\tilde{g}} = 700$ GeV. The case $c = 0$ corresponds to an mSUGRA-like model.

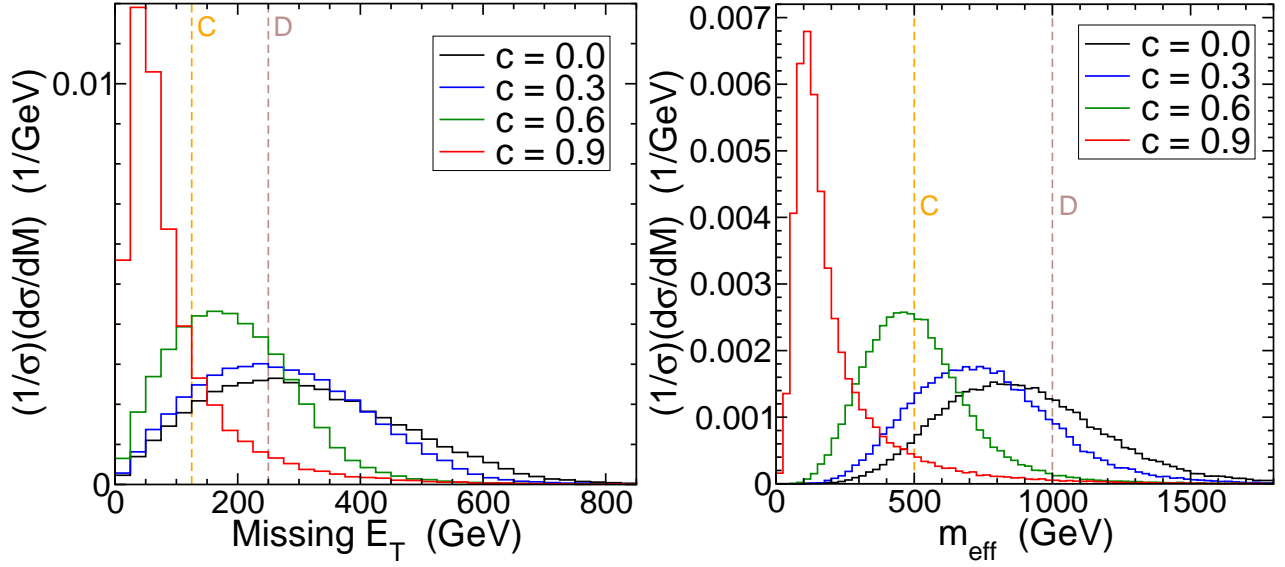


FIG. 2: The distributions before cuts of E_T^{miss} (left panel) and m_{eff} with 3 jets included (right panel) for models described in subsection III A with $M_{\tilde{g}} = 700$ GeV and $c = 0.0, 0.3, 0.6$, and 0.9 , from right to left. The cuts for signals C and D are also shown. The m_{eff} distribution decreases more quickly than E_T^{miss} does as c increases.

LSP, $\tilde{q}_R \rightarrow q\tilde{N}_1$, while left-handed squarks decay mostly to wino-like charginos and neutralinos, $\tilde{q}_L \rightarrow q'\tilde{C}_1$ and $q\tilde{N}_2$. The latter decay through on-shell or off-shell weak bosons: $\tilde{C}_1 \rightarrow W^{(*)}\tilde{N}_1$ and $\tilde{N}_2 \rightarrow Z^{(*)}\tilde{N}_1$, or $\tilde{N}_2 \rightarrow h\tilde{N}_1$ when it is kinematically allowed. The visible energy in each event from these decays clearly decreases as the compression factor c increases, because of the reduction in available kinematic phase space. To illustrate the effect of this, we show in Figure 2 the E_T^{miss} and m_{eff} distributions for $c = 0.0, 0.3, 0.6$, and 0.9 in the case $M_{\tilde{g}} = 700$ GeV. The softening of these distributions becomes drastic as c approaches 1, leading to a more difficult search, at least by the usual methods.

Figure 3 shows the acceptances for signals A, C, D, L for $M_{\tilde{g}} = 300, 400, \dots, 1000$ GeV, with

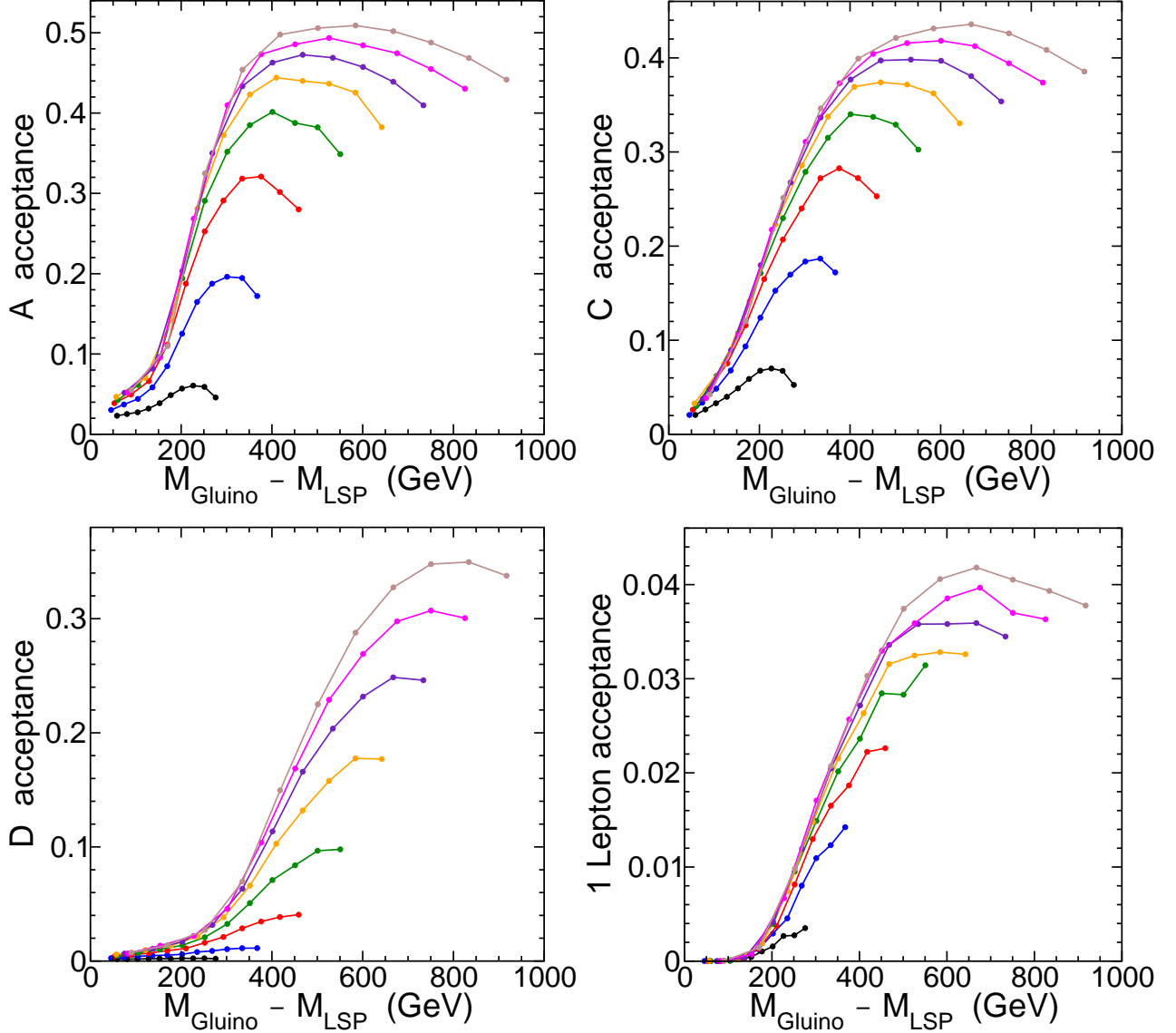


FIG. 3: The acceptances for model lines defined in section III A as a function of $M_{\tilde{g}} - M_{\tilde{N}_1}$, obtained by varying the gaugino mass compression factor c . The lines from bottom to top correspond to $M_{\tilde{g}} = 300, 400, \dots, 1000$ GeV. The dots on each line correspond to, from right to left, $c = -0.1, 0, 0.1, \dots, 0.9$, with $c = 0$ corresponding to the mSUGRA-like case and $c = 1$ to a completely compressed gaugino spectrum. The four panels are for the four sets of cuts A, C, D, and L.

the compression factor varying in the range $-0.1 < c < 0.9$, as a function of the gluino-LSP mass difference $M_{\tilde{g}} - M_{\tilde{N}_1}$. The acceptances for all four signals become sharply reduced when the gluino-LSP mass difference decreases below 200 GeV for the A and C signals, with an even stronger reduction for signals D and L. The single cut most responsible for decreasing the signal in each case is the requirement of a minimum m_{eff} .

An interesting feature seen in Figure 3 is that for fixed $M_{\tilde{g}}$, the acceptances often actually increase with c for low c , especially when $M_{\tilde{g}}$ is large and especially for signals A and C. For a fixed gluino mass, this leads to a maximum acceptance for models that are somewhat more compressed than mSUGRA, which may seem counterintuitive. The interplay between c and the

event kinematics is complicated for cascade decays. The relevant cut is the one on the ratio $E_T^{\text{miss}}/m_{\text{eff}}$; the m_{eff} distribution rapidly becomes softer for increasing c , while the E_T^{miss} distribution decreases much more slowly (and can even increase), allowing more events to pass the ratio cut. This effect can be discerned in Figure 2, for example. (A similar effect was noted in [13].) The events responsible for this effect are those with multi-stage decays of left-handed squarks through the wino-like states \tilde{C}_1 and \tilde{N}_2 , and the largest effect comes specifically from those events in which both winos move in the same direction and both LSPs in the opposite direction relative to a fixed direction perpendicular to the beam. For the component of the signal coming from left-handed squark production, the E_T^{miss} distribution actually becomes significantly harder for increasing c , especially for heavier superpartners. In contrast, for events with single-stage decays $\tilde{q}_R \rightarrow q\tilde{N}_1$, the acceptance decreases monotonically with increasing compression factor c .

Figure 4 shows contours of the total cross section times acceptances for the same models, in the plane of $M_{\tilde{g}}$ and $M_{\tilde{g}} - M_{\tilde{N}_1}$. The dashed line indicates the mSUGRA-like case of $c = 0$, and larger compression factor c occurs lower in each plot. The shaded region corresponds to the case where the LSP is not a neutralino. From this, one infers for example that (to the extent that background levels can be established independent of the signal), if one can set a limit of 850 GeV on $M_{\tilde{g}}$ for mSUGRA-like models in this class with a given set of data using signal D, then the limit would be less than 650 (500) GeV if $M_{\tilde{g}} - M_{\tilde{N}_1}$ is as small as 300 (100) GeV. As a caveat, one might suspect that the more compressed models could also lead to a higher signal contamination of the background control regions, so that the real-world limit would be even weaker, but establishing this effect would require a dedicated background analysis that is beyond the scope of this paper.

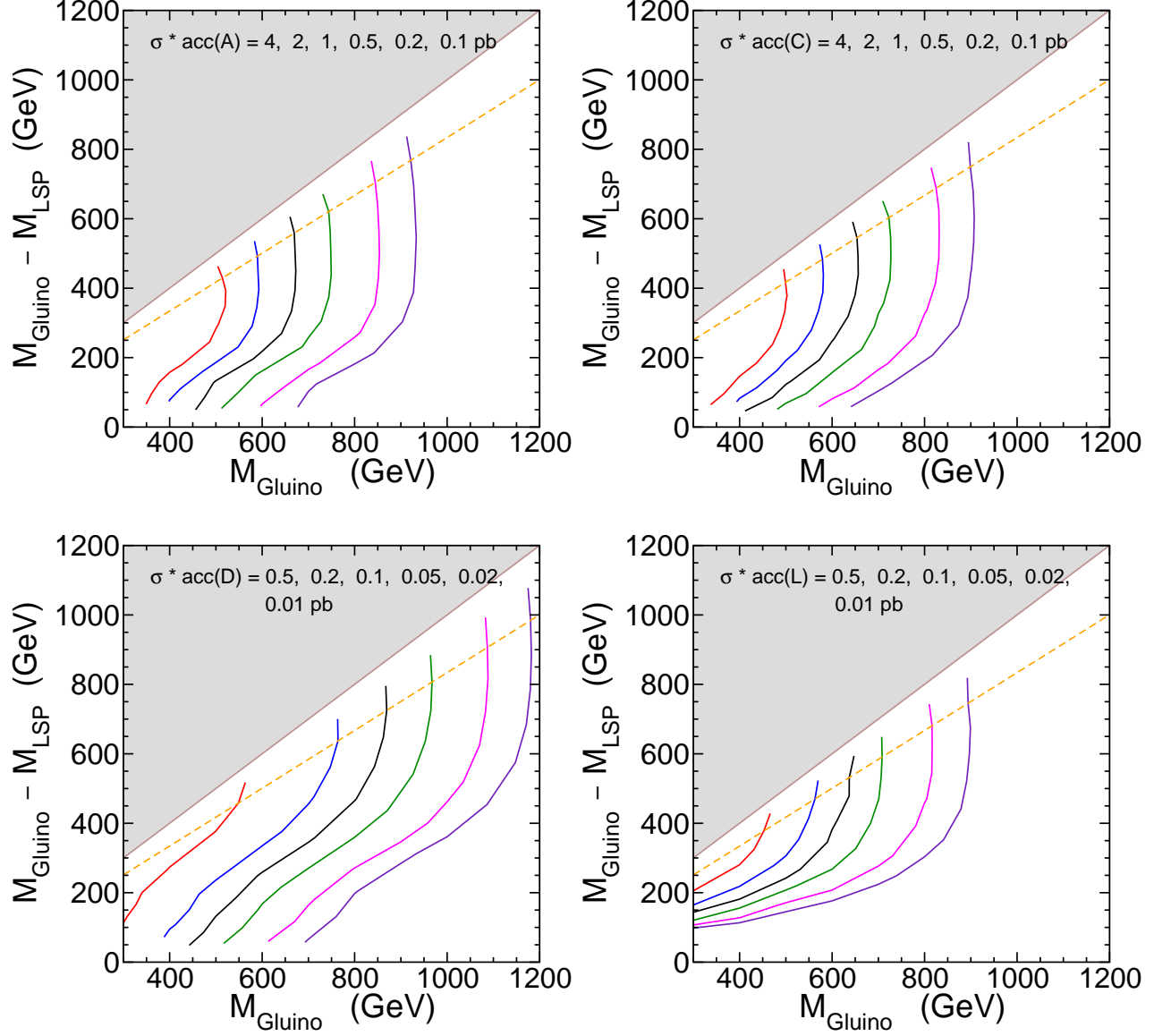


FIG. 4: Contours of cross-section times acceptance for the models defined in section III A, in the $M_{\tilde{g}} - M_{\tilde{N}_1}$ vs. $M_{\tilde{g}}$ plane, obtained by varying the gaugino mass compression parameter c between -0.1 and 0.9 . The dashed line corresponds to the mSUGRA-like case $c = 0$, with increased compression lower in the plane. The four panels correspond to cuts A, C, D, and L.

B. Models with heavy winos

In the models of the previous subsection, the wino-like chargino and neutralino \tilde{C}_1 and \tilde{N}_2 played an important role in the cascade decays of left-handed squarks. In this section, we consider a variation on this class of models in which the wino-like states decouple from LHC phenomenology because they are heavier than the squarks and the gluino. This is never a feature of mSUGRA models, but it is actually motivated [25, 26, 28] as a solution to the supersymmetric little hierarchy problem. The essential reason for this is that in models with a larger ratio M_2/M_3 than in mSUGRA, the renormalization group evolution provides for Higgs potential parameters that require much less tuning to obtain the observed electroweak breaking scale. We therefore consider models just like the ones of the previous section, but with

$$M_1 = \left(\frac{1+5c}{6} \right) M_{\tilde{g}}, \quad (3.3)$$

$$M_2 = M_{\tilde{g}} + 100 \text{ GeV} \quad (3.4)$$

replacing eq. (3.1) at the TeV scale. Thus the gluino-LSP compression is still parameterized by c in the same way as before, but the winos are heavy, so that the most important superpartner masses are just as in Figure 1 with \tilde{N}_2 and \tilde{C}_1 removed. As a result, all first- and second-family squarks now decay directly to the LSP: $\tilde{q} \rightarrow q\tilde{N}_1$. The gluino has direct two-body decays to quarks and squarks as before. This means that signals relying on isolated leptons are absent.[†]

The resulting acceptances for the all-jets signals A, C, D for these heavy-wino models are shown in Figure 5 for $M_{\tilde{g}} = 300, 400, \dots, 1000$ GeV, with the compression factor again varying in the range $-0.1 \leq c \leq 0.9$, as a function of the mass difference $M_{\tilde{g}} - M_{\tilde{N}_1}$. The acceptance for signal L is found to be always extremely small for these models, and so is not shown. Unlike the models in the previous subsection, the acceptance is largest for low compression and decreases (essentially) monotonically for increasing c . This is because of the absence of cascade decays here. At higher compression, the results are qualitatively similar to the light-wino models in the previous subsection, with the main difference being somewhat higher overall acceptances in Figure 5 compared to Figure 3. This can be understood as due to the fact that with direct decays there are more jets with individually high p_T than in the case of cascade decay chains through winos. Nevertheless, in the most compressed limit, there is again very low sensitivity from the signals A, C, and D.

The corresponding cross-section times acceptances are shown in Figure 6, in the plane of $M_{\tilde{g}}$ and $M_{\tilde{g}} - M_{\tilde{N}_1}$ as before. The reach is slightly greater for these heavy wino models in the all-jets signals A,C,D than for the models in subsection III A. We note that although the greatest reach comes from cuts D when the compression is low, the reduction in the signal at high compression is less for cuts A and C. This is because signal D has a much stronger cut on m_{eff} (1000 GeV rather than 500 GeV), and again suggests that an intermediate value for the m_{eff} cut would yield a better

[†] In variations on this type of model with larger $M_{\tilde{g}} - M_{\tilde{t}_1}$, in which decays $\tilde{g} \rightarrow t\tilde{t}_1$ dominate, leptonic signatures from the top decays are important. See subsection III D for an example of this alternative.

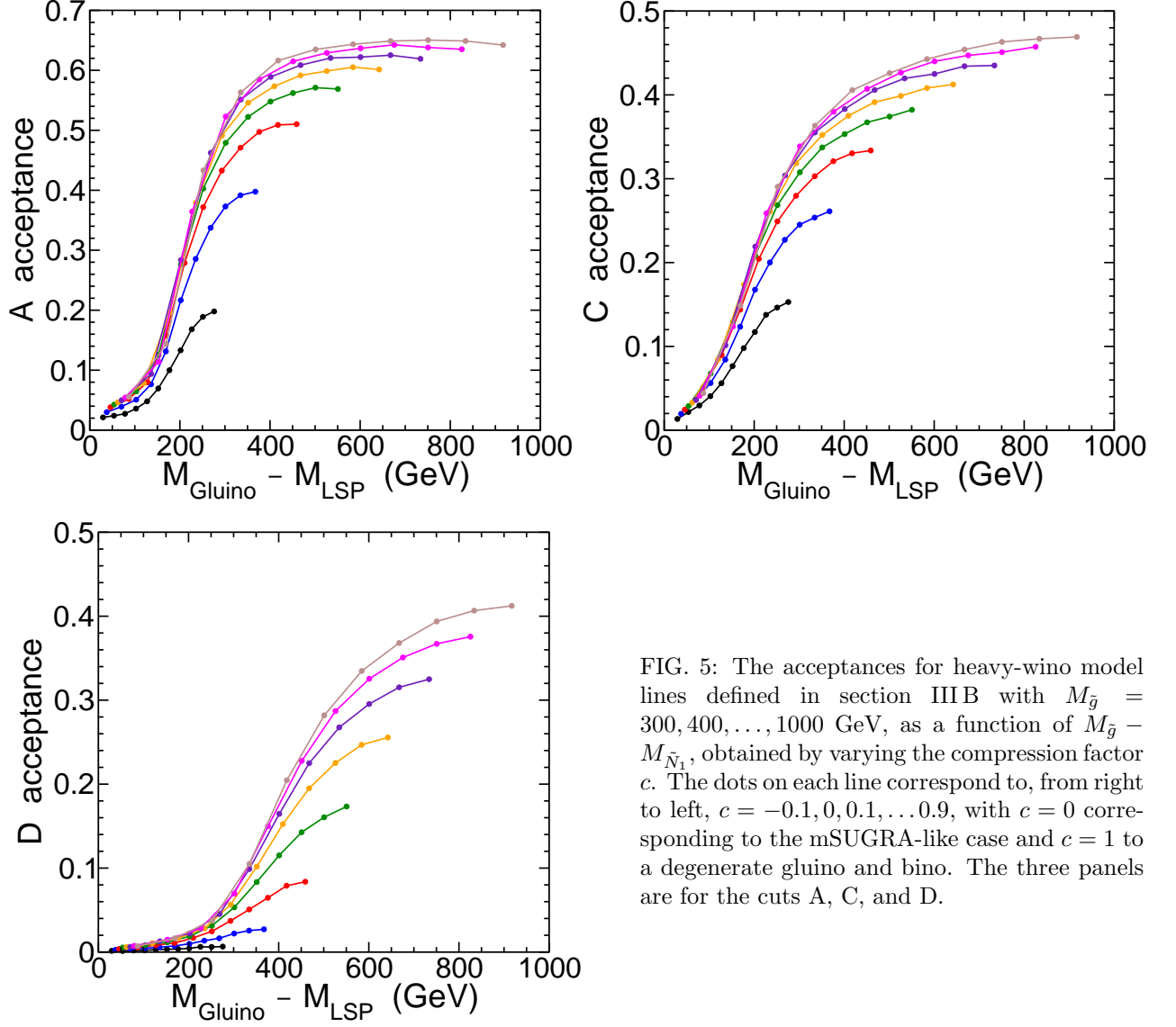


FIG. 5: The acceptances for heavy-wino model lines defined in section IIIB with $M_{\tilde{g}} = 300, 400, \dots, 1000$ GeV, as a function of $M_{\tilde{g}} - M_{\tilde{N}_1}$, obtained by varying the compression factor c . The dots on each line correspond to, from right to left, $c = -0.1, 0, 0.1, \dots, 0.9$, with $c = 0$ corresponding to the mSUGRA-like case and $c = 1$ to a degenerate gluino and bino. The three panels are for the cuts A, C, and D.

reach for compressed SUSY models.

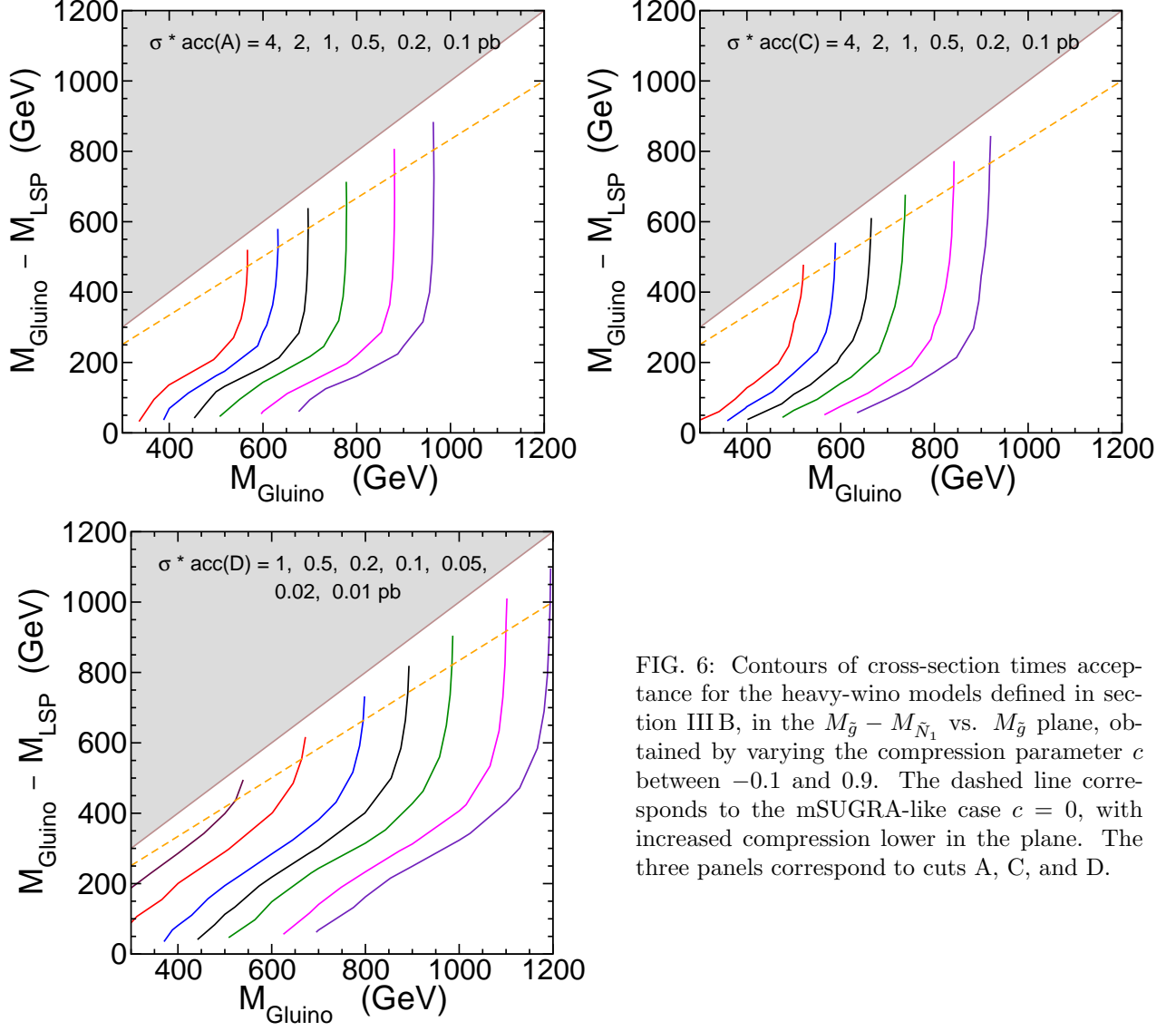


FIG. 6: Contours of cross-section times acceptance for the heavy-wino models defined in section IIIB, in the $M_{\tilde{g}} - M_{\tilde{N}_1}$ vs. $M_{\tilde{g}}$ plane, obtained by varying the compression parameter c between -0.1 and 0.9 . The dashed line corresponds to the mSUGRA-like case $c = 0$, with increased compression lower in the plane. The three panels correspond to cuts A, C, and D.

C. Models with heavy squarks

In the models considered above, the squarks were taken to be lighter than the gluino. However, much heavier squarks may well be motivated by several factors. First, there is the LEP2 constraint on the lightest Higgs scalar boson mass, which increases logarithmically with the top-squark masses. Second, indirect constraints from flavor-violating and CP-violating meson decay and oscillation observables become weaker when squarks are heavier. Third, the so-called focus-point [29, 30] explanation [31] for the WMAP-favored relic abundance of dark matter relies on having heavier squarks.

Therefore, in this section we consider a variation on the models in section III A, but with all squarks taken heavy enough to essentially decouple from the LHC, at least for the purposes of the initial discovery process:

$$m_{\tilde{q}} = M_{\tilde{g}} + 1000 \text{ GeV}. \quad (3.5)$$

The gaugino mass parameters are still related to the compression parameter c as in eq. (3.1), so that the most important superpartner masses are just as depicted in Figure 1 but with the squarks (including \tilde{t}_1) removed. In these models, the most important production cross-section is from gluino pair production, with subsequent gluino decays $\tilde{g} \rightarrow \tilde{C}_1 q \bar{q}'$ and $\tilde{N}_2 q \bar{q}$ and $\tilde{N}_1 q \bar{q}$, with the first two typically dominating. The wino-like states then decay through on-shell or off-shell weak bosons, depending on the mass difference from the compression: $\tilde{C}_1 \rightarrow W^{(*)} \tilde{N}_1$ and $\tilde{N}_2 \rightarrow Z^{(*)} \tilde{N}_1$ or $h \tilde{N}_1$, with the last dominating if kinematically allowed.

The acceptances for signals A, C, D, L are shown in Figure 7, for $M_{\tilde{g}} = 300, 400, \dots, 1000$ GeV, with the compression factor varying in the range $-0.1 \leq c \leq 0.9$, as a function of the mass difference $M_{\tilde{g}} - M_{\tilde{N}_1}$. For each value of the gluino mass, the maximum acceptance occurs at an intermediate compression factor c . This occurs for essentially the same reason as noted in section III A, namely the decays through winos actually have increasingly harder E_T^{miss} distributions with increasing c , as long as c is not too large, and increasingly softer m_{eff} distributions, leading to more events passing the $E_T^{\text{miss}}/m_{\text{eff}}$ ratio cut. In this case, however, it is the gluino cascade decays that provide the effect. Since the production is almost entirely due to gluino pairs, and most gluinos decay through winos, the rise of acceptance with compression for small c is considerably more pronounced than in the models of section III A.

The contours of constant cross-section times acceptance for these heavy squark models are shown in Figure 8. Because squark pair production does not make a significant contribution to the SUSY production, the reach is much weaker than in the models of the previous subsections. The high m_{eff} cut signal D and the single lepton signal L are weak here, and the latter turns off very quickly for higher compression factors (lower in the plane). In fact, only signals A and C provide any reach in the planes shown with $M_{\tilde{g}} > 300$ GeV for the 2010 data set of 35 pb^{-1} at $\sqrt{s} = 7$ TeV. Comparing with the ATLAS limits (see Table I), one sees that the 2010 reach is only up to about $M_{\tilde{g}} = 425$ GeV in the most favorable case, and is less than 350 GeV for the most highly compressed case. We also note again that a cut on m_{eff} that is intermediate between the extremes of 500 GeV

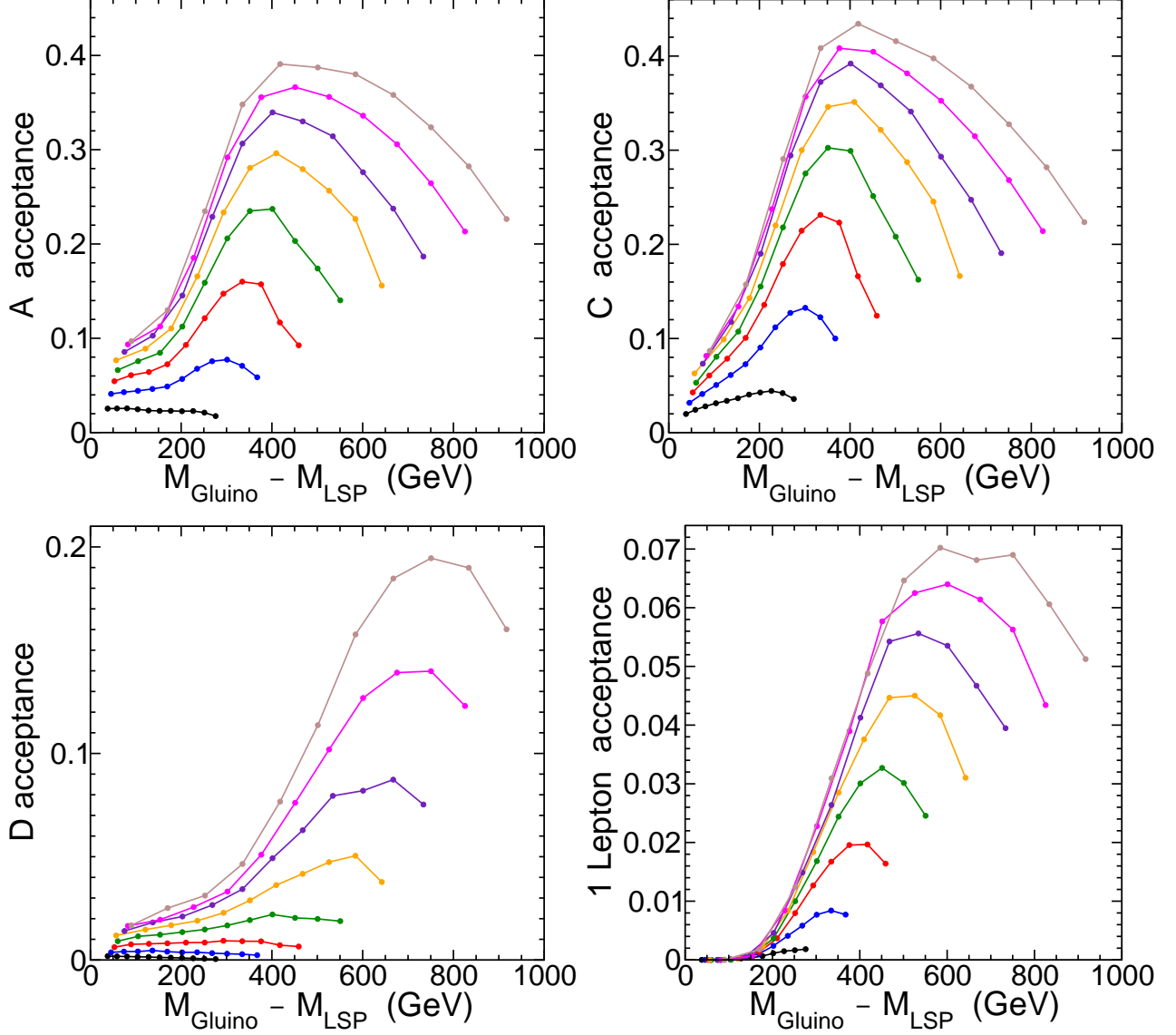


FIG. 7: The acceptances for the heavy squark model lines defined in section III C with $M_{\tilde{g}} = 300, 400, \dots, 1000$ GeV, as a function of $M_{\tilde{g}} - M_{\tilde{N}_1}$, obtained by varying the gaugino mass compression factor c . The dots on each line correspond to, from right to left, $c = -0.1, 0, 0.1, \dots, 0.9$, with $c = 0$ corresponding to the mSUGRA-like case and $c = 1$ to a completely compressed gaugino spectrum. The four panels are for the four sets of cuts A, C, D, and L.

(C) and 1000 GeV (D) may be more efficient in setting future limits or making a discovery.

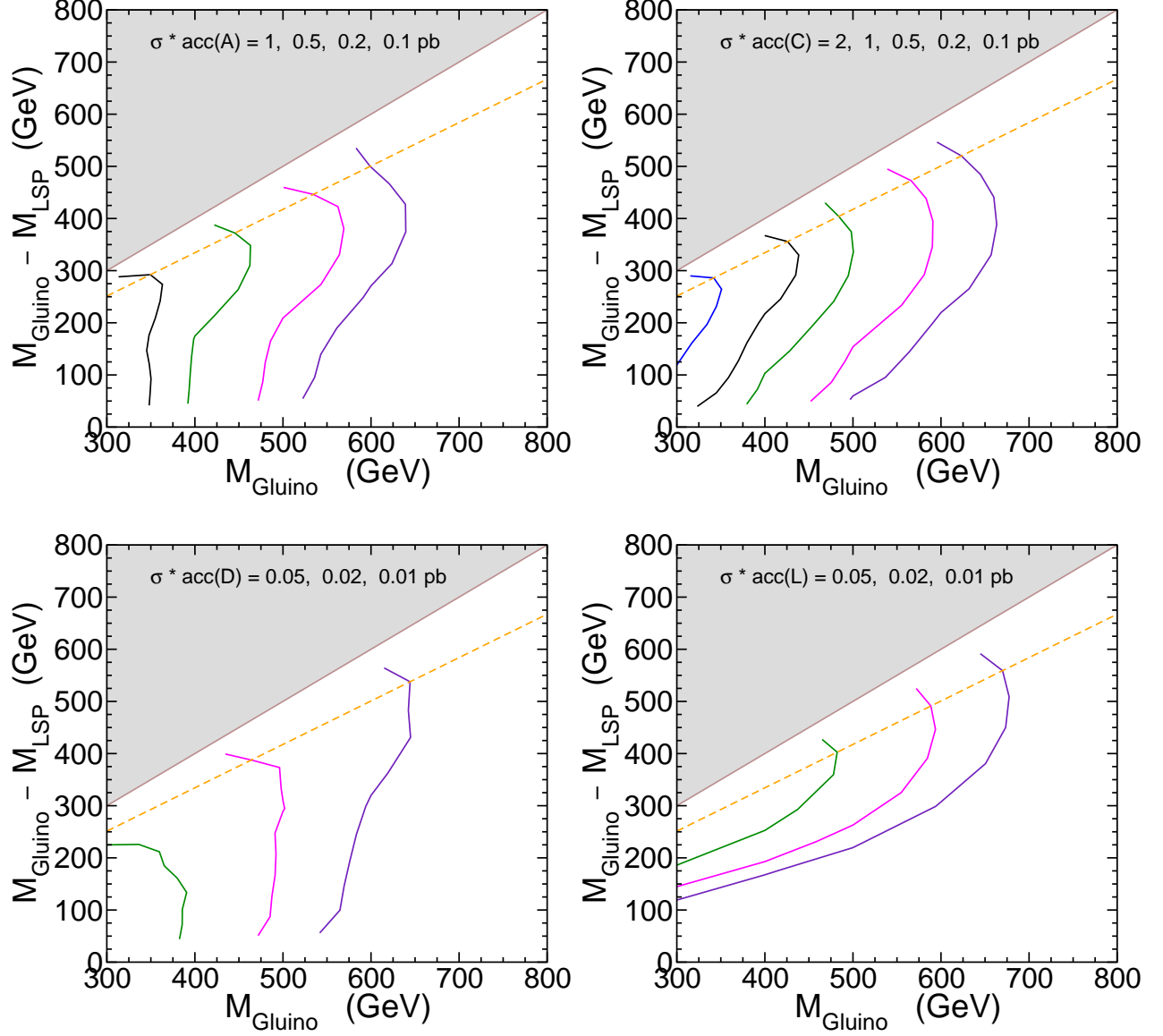


FIG. 8: Contours of cross-section times acceptance for the heavy-squark models defined in section III C, in the $M_{\tilde{g}} - M_{\tilde{N}_1}$ vs. $M_{\tilde{g}}$ plane, obtained by varying the compression parameter c between -0.1 and 0.9 . The dashed line corresponds to the mSUGRA-like case $c = 0$, with increased compression lower in the plane. The four panels correspond to cuts A, C, D, and L.

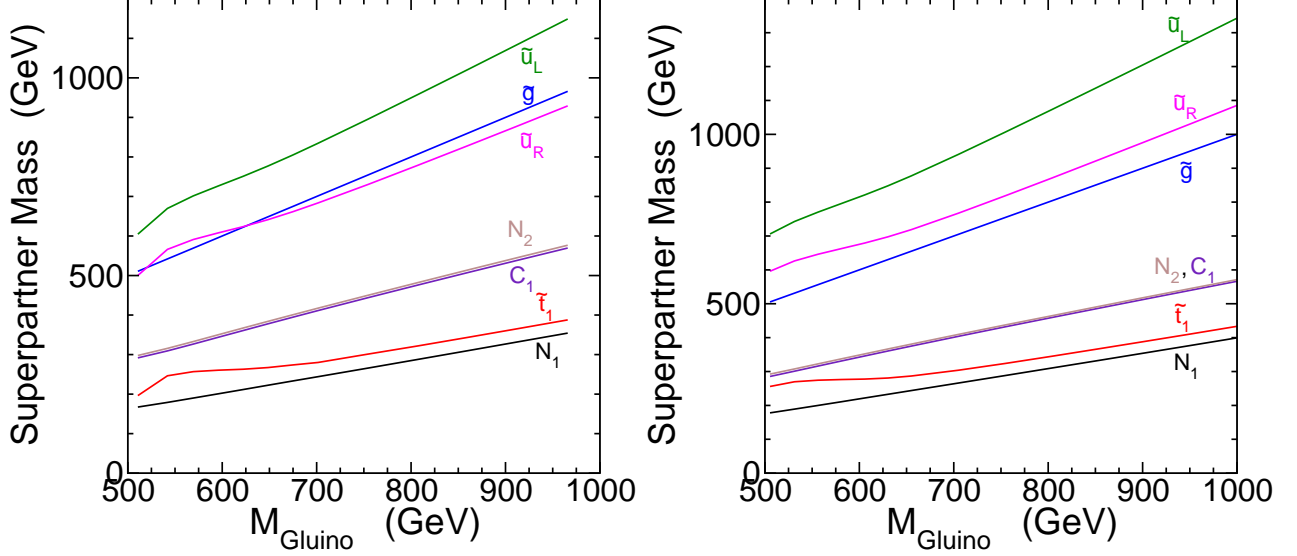


FIG. 9: The masses of important superpartners for models with $C_{24} = 0.21$ (left panel) and $C_{24} = 0.23$ (right panel), for varying $M_1 = -A_0$, with $\tan \beta = 10$, $\mu > 0$, with m_0 determined by requiring $\Omega_{\text{DM}} h^2 = 0.11$.

D. Models with light stops motivated by dark matter

In this subsection, we will consider a class of models proposed previously in [25, 26] as a simultaneous solution to the supersymmetric little hierarchy problem and the problem of obtaining a relic density of dark matter in agreement with WMAP and other astrophysics data [27]. These models generalize mSUGRA to include non-universal gaugino masses in a pattern corresponding to an F -term VEV in an adjoint representation (rather than a singlet) of the global $SU(5)$ group that contains the Standard Model gauge group. Gaugino masses are parameterized by:

$$M_1 = m_{1/2}(1 + C_{24}) \quad M_2 = m_{1/2}(1 + 3C_{24}) \quad M_3 = m_{1/2}(1 - 2C_{24}), \quad (3.6)$$

at M_{GUT} , with $C_{24} = 0$ corresponding to mSUGRA and $C_{24} > 0$ to compressed SUSY. For $C_{24} \sim 0.18$ to 0.28 , the lighter top squark can be the next-to-lightest superpartner, and the WMAP-favored relic abundance of dark matter is achieved by efficient annihilations $\tilde{N}_1 \tilde{N}_1 \rightarrow t\bar{t}$, mediated by \tilde{t}_1 in the t -channel, provided that $m_t \lesssim m_{\tilde{N}_1} \lesssim m_t + 100$ GeV. (The region of parameter space where this occurs is continuously connected to the more fine-tuned case of stop coannihilation with dark matter.) The other parameters are as in mSUGRA; we will use $A_0 = -M_1$, $\tan \beta = 10$, $\mu > 0$, and m_0 chosen so as to obtain $\Omega_{\text{DM}} h^2 = 0.11$. (In this section, we adopt a different attitude towards the thermal dark matter density than in previous sections by enforcing this requirement.) The masses of the most relevant superpartners are shown in Figure 9, for the choices $C_{24} = 0.21$ and 0.23 . For brevity, we chose here to consider only these two values of C_{24} , because at a qualitative level many of the issues that impact the signal are similar to those found in the previous sections.

In these models, the gluino decays according to $\tilde{g} \rightarrow t\bar{t}_1^*$ and $\tilde{g} \rightarrow \bar{t}t_1$ each 50%. In turn, the lighter

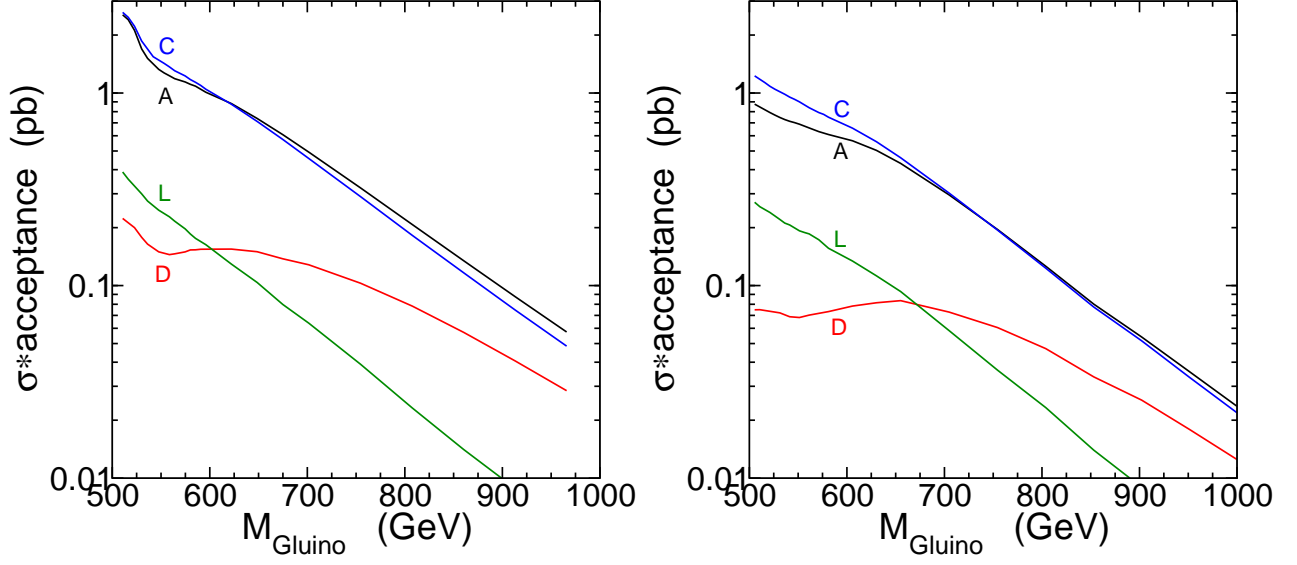


FIG. 10: The cross-section times acceptance for the same model lines in Figure 9, as a function of the gluino mass, for the four sets of cuts A, C, D, and L.

top squark decays 100% according to $\tilde{t}_1 \rightarrow c\tilde{N}_1$, a flavor-violating 2-body decay.[†] Although the pair production of light stops has the largest cross-section of all SUSY processes at the LHC, it has a very low acceptance for all signals considered here, due to the small kinematic phase space of this decay; the charm jets typically have very low p_T . The first- and second-family squarks decay mostly according to $\tilde{q}_L \rightarrow q\tilde{g}$ and $q_R \rightarrow q\tilde{N}_1$, with subdominant decays to the neutralinos and charginos \tilde{N}_2, \tilde{N}_3 and \tilde{C}_1 , which are higgsino-like in these models. (The wino-like states are heavier and essentially decouple.)

The compression of the spectrum in these dark-matter motivated models is not extreme, with a ratio $M_{\tilde{g}}/M_{\tilde{N}_1}$ of roughly 2.7 for the $C_{24} = 0.21$ model line and 2.9 for the $C_{24} = 0.23$ model line, corresponding roughly to compression factors of $c = 0.21$ and $c = 0.25$ in the language of section III A. The most striking qualitatively different feature is the presence of top quarks in all decays involving the gluino.[‡]

The cross-section times acceptance for signals A, C, D, and L for these model lines is shown in Figure 10 as a function of the gluino mass. As might be expected from the results of the previous section, the moderate compression of the spectrum in these examples is not enough to strongly deplete the signal. For the $C_{24} = 0.21$ model line, the 2010 ATLAS bounds in Table I should exclude up to $M_{\tilde{g}} = 575$ GeV with signal C (although this should be considered approximate in the absence of a dedicated study of backgrounds and detectors responses), and perhaps about the same from signal L (taking into account the fact, mentioned at the end of section II above, that our methodology tends to give 20% to 50% larger acceptances for the 1-lepton channel than were reported by ATLAS). The exclusion obtainable from signal D is hard to estimate, as the cross-

[†] It is also possible that the 4-body decay $\tilde{t}_1 \rightarrow bf\tilde{f}'\tilde{N}_1$ is competitive [32]. We assume that there is sufficient flavor violation in the soft supersymmetry breaking sector to assure that the 2-body decay wins and is prompt.

[‡] Since the gluino is Majorana, the charges of the two top quarks in each event are uncorrelated, leading to a rare but very low-background same-sign top-quark signal, not explored here. See for example refs. [33] and [26].

section times acceptance is relatively flat over a large range of gluino masses, but it may already be above $M_{\tilde{g}} = 725$ GeV with 2010 data. Obtaining a real estimate of the exclusion would require a dedicated analysis of the backgrounds and detector responses. The $C_{24} = 0.23$ model line has weaker signals, due to having heavier squarks. Here, the signal D is not quite able to exclude any models along the line, and the signal L reach is the best but with 2010 data does not extend much beyond $M_{\tilde{g}} = 600$ GeV.

Fortunately, with the greater integrated luminosity to become available soon, these models will be confronted out to much larger gluino masses. For high masses, the signal D appears to have the best sensitivity, out of the ones considered here, but it is likely that modified sets of cuts will do even better. In particular, the large multiplicity of jets in the two top decays suggests that m_{eff} would be better replaced by a variable that summed over more jets, to better capture the distinction between these events and QCD backgrounds. Also, bottom tagging could be helpful.

IV. OUTLOOK

In this paper, we have studied the reach of the $\sqrt{s} = 7$ TeV LHC for supersymmetric models with compressed mass spectra. Such models are not just interesting ways to hide SUSY, but can be motivated as providing a solution to the supersymmetric little hierarchy problem. We found that with mild to moderate compression, the acceptances are good and sometimes even much better than in mSUGRA. Acceptances drastically decrease for more severe compression, as expected due to the low visible energy in each event. The m_{eff} cut is typically more damaging to the signal than the E_T^{miss} cut, but even for the most extreme compression there is some reach in the multi-jet channels. For high compression, the 1-lepton signal goes away completely, due to the difficulty in getting high p_T leptons and large transverse mass m_T from decays with small mass differences.

These studies suggest that signals with an intermediate (between the extremes of 500 and 1000 GeV) cut on m_{eff} might be more useful in extending the reach. Also, signals that cut on kinematic variables that augment m_{eff} by involving more than 3 jets may be better at probing signals from models with 3-body and cascade decays. A question that should be addressed in future analyses is whether compressed SUSY might contribute to QCD background control regions (used to estimate background from data) in dangerous way. We look forward to the data currently being gathered at the LHC probing supersymmetry in large regions of parameter space by using comprehensive search strategies involving a variety of different signals.

Acknowledgments: We thank Johan Alwall, Jerry Blazey, Jay Wacker, and Adam Yurkewicz for useful conversations. The work of TJL was supported in part by the U.S. Department of Energy, Division of High Energy Physics, under Contract DE-AC02-06CH11357. The work of SPM was supported in part by the National Science Foundation grant number PHY-0757325.

-
- [1] The ATLAS collaboration, “ATLAS Detector and physics performance technical design report”, Volume 2. CERN-LHCC-99-15, ATLAS-TDR-15, May 1999.
 - [2] The CMS collaboration, “CMS Physics Technical Design Report”, Volume 1, Detector Performance and Software. CERN-LHCC-2006-001, CMS TDR 8.1, February 2006.
 - [3] For reviews of supersymmetry at the TeV scale, see S.P. Martin, “A supersymmetry primer,” [hep-ph/9709356] (version 5, December 2008). M. Drees, R. Godbole and P. Roy, “Theory and phenomenology of sparticles: An account of four-dimensional N=1 supersymmetry in high energy physics,”

- World Scientific (2004)*. H. Baer and X. Tata, “Weak scale supersymmetry: From superfields to scattering events,” *Cambridge University Press (2006)*.
- [4] G. Aad *et al.* [ATLAS Collaboration], “Search for supersymmetry using final states with one lepton, jets, and missing transverse momentum with the ATLAS detector in $\sqrt{s} = 7$ TeV pp,” [1102.2357 [hep-ex]].
 - [5] G. Aad *et al.* [ATLAS Collaboration], “Search for squarks and gluinos using final states with jets and missing transverse momentum with the ATLAS detector in $\sqrt{s} = 7$ TeV proton-proton collisions,” [1102.5290 [hep-ex]].
 - [6] G. Aad *et al.* [ATLAS Collaboration], “Search for supersymmetry in pp collisions at $\sqrt{s} = 7$ TeV in final states with missing transverse momentum and b-jets,” [1103.4344 [hep-ex]].
 - [7] G. Aad *et al.* [ATLAS Collaboration], “Search for supersymmetric particles in events with lepton pairs and large missing transverse momentum in $\sqrt{s} = 7$ TeV proton-proton collisions with the ATLAS experiment,” [1103.6214 [hep-ex]].
 - [8] V. Khachatryan *et al.* [CMS Collaboration], “Search for Supersymmetry in pp Collisions at 7 TeV in Events with Jets and Missing Transverse Energy,” *Phys. Lett. B* **698**, 196 (2011) [1101.1628 [hep-ex]].
 - [9] S. Chatrchyan *et al.* [CMS Collaboration], “Search for Physics Beyond the Standard Model in Opposite-Sign Dilepton Events at $\sqrt{s} = 7$ TeV,” 1103.1348 [hep-ex].
 - [10] S. Chatrchyan *et al.* [CMS Collaboration], “Search for new physics with same-sign isolated dilepton events with jets and missing transverse energy at the LHC,” 1104.3168 [hep-ex].
 - [11] H. Baer, D. Karatas and X. Tata, *Phys. Lett. B* **183**, 220 (1987).
 - [12] H. Baer, A. Box, E.K. Park and X. Tata, *JHEP* **0708**, 060 (2007) 0707.0618 [hep-ph].
 - [13] D.S.M. Alves, E. Izaguirre and J.G. Wacker, “It’s On: Early Interpretations of ATLAS Results in Jets and Missing Energy Searches,” 1008.0407 [hep-ph];
 - [14] J.A. Conley, J.S. Gainer, J.L. Hewett, M.P. Le and T.G. Rizzo, “Supersymmetry without prejudice at the LHC,” 1009.2539 [hep-ph]; “Supersymmetry without prejudice at the 7 TeV LHC,” 1103.1697 [hep-ph].
 - [15] S. Scopel, S. Choi, N. Fornengo and A. Bottino, 1102.4033 [hep-ph].
 - [16] O. Buchmueller *et al.*, *Eur. Phys. J. C* **71**, 1634 (2011) 1102.4585 [hep-ph]. See also P. Bechtle *et al.*, arXiv:1102.4693 [hep-ph] for a similar study within mSUGRA.
 - [17] D.S.M. Alves, E. Izaguirre and J.G. Wacker, “Where the Sidewalk Ends: Jets and Missing Energy Search Strategies for the 7 TeV LHC,” 1102.5338 [hep-ph].
 - [18] S. Akula, D. Feldman, Z. Liu, P. Nath and G. Peim, “New Constraints on Dark Matter from CMS and ATLAS Data,” 1103.5061 [hep-ph].
 - [19] J. Alwall *et al.*, *JHEP* **0709**, 028 (2007) F. Maltoni and T. Stelzer, “MadEvent: Automatic event generation with MadGraph,” *JHEP* **0302**, 027 (2003) [hep-ph/0208156], T. Stelzer and W. F. Long, *Comput. Phys. Commun.* **81**, 357 (1994) [hep-ph/9401258].
 - [20] J. Pumplin *et al.*, *JHEP* **0207**, 012 (2002) [hep-ph/0201195].
 - [21] T. Sjostrand, S. Mrenna and P. Skands, *JHEP* **0605**, 026 (2006) [hep-ph/0603175].
 - [22] John Conway *et al.*, “PGS4: Pretty Good Simulation of high energy collisions”, <http://www.physics.ucdavis.edu/~conway/research/software/pgs/pgs4-general.htm>.
 - [23] <http://cp3wks05.fynu.ucl.ac.be/twiki/bin/view/Main/IntroMatching>. See also J. Alwall, S. de Visscher and F. Maltoni, *JHEP* **0902**, 017 (2009) 0810.5350 [hep-ph]. J. Alwall *et al.*, *Eur. Phys. J. C* **53**, 473 (2008) 0706.2569 [hep-ph].
 - [24] Prospino 2.1, available at <http://www.ph.ed.ac.uk/~tplehn/prospino/>, uses results found in: W. Beenakker, R. Hopker, M. Spira and P.M. Zerwas, *Nucl. Phys. B* **492**, 51 (1997) [hep-ph/9610490], W. Beenakker *et al.*, *Nucl. Phys. B* **515**, 3 (1998) [hep-ph/9710451], W. Beenakker *et al.*, *Phys. Rev. Lett.* **83**, 3780 (1999) [Erratum-ibid. **100**, 029901 (2008)] [hep-ph/9906298], M. Spira, [hep-ph/0211145], T. Plehn, *Czech. J. Phys.* **55**, B213 (2005) [hep-ph/0410063].
 - [25] S.P. Martin, *Phys. Rev. D* **75**, 115005 (2007) [hep-ph/0703097], *Phys. Rev. D* **76**, 095005 (2007) [hep-ph/0707.2812].
 - [26] S.P. Martin, *Phys. Rev. D* **78**, 055019 (2008). 0807.2820 [hep-ph].
 - [27] E. Komatsu *et al.* [WMAP Collaboration], *Astrophys. J. Suppl.* **192**, 18 (2011) 1001.4538 [astro-ph.CO].
 - [28] G.L. Kane and S.F. King, *Phys. Lett. B* **451**, 113 (1999) [hep-ph/9810374], M. Bastero-Gil, G.L. Kane and S.F. King, *Phys. Lett. B* **474**, 103 (2000) [hep-ph/9910506].
 - [29] K.L. Chan, U. Chattopadhyay and P. Nath, *Phys. Rev. D* **58**, 096004 (1998) [hep-ph/9710473].
 - [30] J.L. Feng, K.T. Matchev and T. Moroi, *Phys. Rev. Lett.* **84**, 2322 (2000) [hep-ph/9908309]; *Phys. Rev. D* **61**, 075005 (2000) [hep-ph/9909334].
 - [31] J.L. Feng, K.T. Matchev and F. Wilczek, *Phys. Lett. B* **482**, 388 (2000) [hep-ph/0004043].
 - [32] K.-i. Hikasa, M. Kobayashi, *Phys. Rev. D* **36**, 724 (1987) C. Boehm, A. Djouadi and Y. Mambrini, *Phys. Rev. D* **61**, 095006 (2000) [hep-ph/9907428]. S.P. Das, A. Datta and M. Guchait, *Phys. Rev. D* **65**, 095006 (2002) [hep-ph/0112182]. G. Hiller and Y. Nir, *JHEP* **0803**, 046 (2008) [0802.0916 [hep-ph]]. A.D. Box and X. Tata, *Phys. Rev. D* **79**, 035004 (2009) [Erratum-ibid. **D 82**, 119905 (2010)] 0810.5765 [hep-ph]. M. Muhlleitner and E. Poppo, *JHEP* **1104**, 095 (2011) 1102.5712 [hep-ph].
 - [33] S. Kraml and A.R. Raklev, *Phys. Rev. D* **73**, 075002 (2006) [hep-ph/0512284].